TECHNICAL PROGRESS REPORT

For the Period Ending 09-30-06
(April 1, 2006 to September 30, 2006)

Award Number DE-FC26-03NT41964

Sponsor: DOE Pittsburgh Energy Technology Center

Design, Synthesis, and Mechanistic Evaluation of Iron-Based Catalysis for Synthesis Gas Conversion to Fuels and Chemicals

Akio Ishikawa, Manuel Ojeda, Nan Yao, and Enrique Iglesia
Department of Chemical Engineering
University of California at Berkeley
Berkeley, CA 94720

DISCLAIMER:

ABSTRACT

This project extends previously discovered Fe-based catalysts to hydrogen-poor synthesis gas streams derived from coal and biomass sources. These catalysts have shown unprecedented Fischer-Tropsch synthesis rates and selectivities for feedstocks consisting of synthesis gas derived from methane. During the first reporting period, we certified a microreactor, installed required analytical equipment, and reproduced synthetic protocols and catalytic results previously reported. During the second reporting period, we prepared several Fe-based compositions for Fischer-Tropsch Synthesis and tested the effects of product recycle under both subcritical and supercritical conditions. During the third and fourth reporting periods, we improved the catalysts preparation method, which led to Fe-based FT catalysts with the highest FTS reaction rates and selectivities so far reported, a finding that allowed their operation at lower temperatures and pressures with high selectivity to desired products (C_{5+}, olefins). During the fifth reporting period, we studied the effects of different promoters on catalytic performance, specifically how their sequence of addition dramatically influenced the performance of these materials in the Fischer-Tropsch synthesis. We also continued our studies of the kinetic behavior of these materials. Specifically, the effects of H_2, CO, and CO_2 on the rates and selectivities of Fischer-Tropsch Synthesis reactions led us to propose a new sequence of elementary steps on Fe and Co Fischer-Tropsch catalysts. More specifically, we were focused on the roles of hydrogen-assisted and alkali-assisted dissociation of CO in determining rates and CO_2 selectivities.

During this sixth reporting period, we have studied the validity of the mechanism that we propose by analyzing the H_2/D_2 kinetic isotope effect (r_H/r_D) over a conventional iron-based Fischer-Tropsch catalyst Fe-Zn-K-Cu. We have observed experimentally that the use of D_2 instead of H_2 leads to higher hydrocarbons formation rates (inverse kinetic isotopic effect). On the contrary, primary carbon dioxide formation is not influenced. These experimental observations can be explained by the two CO activation pathways we propose. During this reporting period, the experimental kinetic study has been also complemented with periodic, self-consistent, DFT-GGA investigations in a parallel collaboration with the group of Manos Mavrikakis at the University of Wisconsin-Madison. These DFT calculations suggest minimal energy paths for proposed elementary steps on Fe(110) and Co(0001) surfaces. These calculations support our novel conclusions about the preferential dissociation of CO dissociation via H-assisted pathways on Fe-based catalysts. Unassisted CO dissociation also occurs and lead to the formation of CO_2 as a primary oxygen scavenging mechanism after CO dissociation on Fe-based catalysts. Simulations and our experimental data show also that unassisted CO dissociation route is much less likely on Co surfaces and that hydrocarbons form exclusively via H-assisted pathways with the formation of H_2O as the sole oxygen rejection product.

We have also started a study of the use of colloidal precipitation methods for the synthesis of small Fe and Co clusters using recently developed methods to explore possible further improvements in Fischer-Tropsch synthesis rates and selectivities. We have found that colloidal synthesis makes possible the preparation of small cobalt particles, although large amount of cobalt silicate species, which are difficult to reduce, are formed. The nature of the cobalt precursor and the modification of the support seem to be critical parameters in order to obtain highly dispersed and reducible Co nanoparticles.

TABLE OF CONTENTS

TITLE PAGE 1
DISCLAIMER 2
ABSTRACT 3
TABLE OF CONTENTS 4
EXECUTIVE SUMMARY 5
OBJECTIVES AND SPECIFIC TASKS 7
TECHNICAL ACTIVITIES AND ACCOMPLISHMENTS 8
APPENDIX A:
1. EXPERIMENTAL DETAILS 10
1.1. Synthesis of precursors and catalysts 10
1.2. Catalysts characterization 12
1.3. Fischer-Tropsch Synthesis activity and selectivity 12
2. RESULTS AND DISCUSSION
2.1. Catalytic performance of Fe-Zn-Cu_3-K_6 in the Fischer-Tropsch Synthesis 12
2.2. Kinetic study of the Fischer-Tropsch Synthesis 15
2.2.1. Mechanism and kinetics 15
2.2.2. Kinetic H_2/D_2 isotope effects on Fe-based catalysts 16
2.2.3. *Theoretical calculations for the Fischer-Tropsch Synthesis mechanism* 19
2.3. Metallic colloids for Fischer-Tropsch Synthesis catalysts 19
2.3.1. Effect of SiO_2 modification with ZrO_2 19
2.3.2. Effect of colloid method 21
APPENDIX B:
1. Publications 24
2. Presentations and Abstracts 24

EXECUTIVE SUMMARY

This project exploits our recent discovery of catalyst compositions and synthesis and activation protocols leading to iron-based catalysts with Fischer-Tropsch synthesis (FTS) rates and selectivities similar to those on cobalt-based catalyst at low temperatures required to form olefins and large hydrocarbons using stoichiometric synthesis gas. These materials are being extended to the conversion of substoichiometric streams to explore whether the unprecedented activities and selectivities with streams derived from natural gas can be realized with more demanding coal-derived synthesis gas ratios. Fe catalysts convert streams derived from coal and biomass, because O-atoms are rejected as CO_2 instead of H_2O, but they tend to be much less active than Co catalysts, which reject O-atoms as H_2O. Fe catalysts are often less stable, because phase transformations can lead to structural disintegration. Higher FTS rates, lower CO_2 selectivities, and greater structural stability remain critical hurdles in converting H_2-poor streams to high-value fuels and chemicals. During the first reporting period, we certified a microreactor, installed required analytical tools, and reproduced previous synthetic protocols and catalytic results. During the second reporting period, we prepared several Fe-based compositions for Fischer-Tropsch synthesis and tested the effects of product recycle under both subcritical and supercritical conditions. During the third reporting period, we improved catalyst synthesis protocols, and achieved the highest FTS reaction rates and selectivities so far reported at the low temperatures required for selectivity and stability. During the fourth and in this fifth reporting period, we have studied the effects of different promoters on catalytic performance, specifically how their sequence of addition dramatically influences the performance of these materials in the Fischer-Tropsch synthesis. The resulting procedures have been optimized to improve further upon the already unprecedented rates and C_{5+} selectivities of the Fe-based catalysts that we have developed as part of this project.

During this sixth reporting period, we have studied the validity of the mechanism that we propose by analyzing the H_2/D_2 kinetic isotope effect (r_H/r_D) over a conventional iron-based Fischer-Tropsch catalyst Fe-Zn-K-Cu. We have observed experimentally that the use of D_2 instead of H_2 leads to higher hydrocarbons formation rates (inverse kinetic isotopic effect). On the contrary, primary carbon dioxide formation is not influenced. These experimental observations can be explained by the two CO activation pathways we propose. During this reporting period, the experimental kinetic study has been also complemented with periodic, self-consistent, DFT-GGA investigations in a parallel collaboration with the group of Manos Mavrikakis at the University of Wisconsin-Madison. These DFT calculations suggest minimal energy paths for proposed elementary steps on Fe(110) and Co(0001) surfaces. These calculations support our novel conclusions about the preferential dissociation of CO dissociation via H-assisted pathways on Fe-based catalysts. Unassisted CO dissociation also occurs and lead to the formation of CO_2 as a primary oxygen scavenging mechanism after CO dissociation on Fe-based catalysts. Simulations and our experimental data show also that unassisted CO dissociation route is much less likely on Co surfaces and that hydrocarbons form exclusively via H-assisted pathways with the formation of H_2O as the sole oxygen rejection product.

We have also started a study of the use of colloidal precipitation methods for the synthesis of small Fe and Co clusters using recently developed methods to explore possible further improvements in Fischer-Tropsch synthesis rates and selectivities. We have found that colloidal synthesis makes possible the preparation of small cobalt particles, although large amount of cobalt silicate species, which are difficult to reduce, are formed. The nature of the cobalt precursor and the modification of the support seem to be critical parameters in order to obtain highly dispersed and reducible Co nanoparticles.

Design, Synthesis, and Mechanistic Evaluation of Iron-Based Catalysis for Synthesis Gas Conversion to Fuels and Chemicals

Description of Tasks

Task One (Years 1 and 2)
Extension of synthesis and activating protocols for Fe-based catalysts prepared by precipitation, treatment with surface-active agents, activation in synthesis gas, and promotion by Ru to materials suitable Fischer-Tropsch synthesis with coal- and biomass-derived synthesis gas.

Task Two (Years 1 and 2)
Characterization of carbide-oxide phase transformations and their impact on catalyst mechanical integrity using electron microscopy and in situ X-ray absorption protocols.

Task Three (Years 2 and 3)
Exploratory studies of the effects of CO_2 and light hydrocarbon recycle on the rate and selectivity of FTS reactions at low H_2/CO ratios on optimized Fe-based catalysts (developed in part (i)).

Objectives and Specific Tasks

Fe-based catalysts are typically preferred for converting coal or biomass derived synthesis gas streams with low H_2/CO ratios (H_2/CO = 0.7-1) because their significant water-gas shift activity ($H_2O + CO \rightarrow CO_2 + H_2$) leads to rejection of excess carbon as CO_2. Fe-based catalysts typically show much lower catalytic activities than Co-based catalysts and lower mechanical stability, as a result of their tendency to interconvert between oxide and carbide phases as the redox properties change within catalytic reactors. Fe-based catalysts with higher Fischer-Tropsch Synthesis (FTS) activity and greater structural integrity remain significant obstacles to their use in the synthesis of high-value fuels and petrochemicals.

Iron-based catalysts with FTS activities and selectivities similar to those on cobalt-based catalyst using stoichiometric H_2/CO streams derived from natural gas were recently reported by our research group. Novel synthesis methods based on supercritical and subcritical drying of powders after precipitation at a constant pH led to significant improvements in the surface area of oxide precursors, while activation and promotion protocols led to active Fe carbide clusters with high surface areas and mechanical strength. These gave in turn unprecedented activity and C_{5+} selectivity during use with stoichiometric synthesis gas (H_2/CO = 2).

The principal objectives of this project are to:

1. optimize synthesis protocols to prepare Fe-based catalysts with FTS rates and hydrocarbon product distributions similar to those of Co-based materials using surface-active compounds and supercritical conditions and explore the use of Ru as activation promoter,

2. evaluate the performance of prepared catalysts in synthesis gas streams derived from coal or biomass ($H_2/CO = 0.7\text{-}1.0$) and optimize activation protocols for high activity, selectivity and mechanical integrity,

3. determine the effects of Ru loading and mode of addition on the concentration of active sites and on the intrinsic activity and selectivity of such active sites,

4. establish the extent and dynamics of carbide-oxide transformations during reactions of synthesis gas mixtures with varying redox potential and their influence on the structural integrity and stability of Fe-based catalysts.

Technical Activities and Accomplishments (FY 2006)

During the fifth and sixth reporting periods, covering Fiscal Year 2006, we have prepared and characterized some Fe-based catalyst and we have measured their Fischer-Tropsch synthesis reaction rates and selectivities. These studies have:

(1) established an appropriate method of iron-based catalysts promotion, resulting in the improvement of the catalytic activity compared to the previous work,
(2) performed the evaluation of the performance of prepared catalysts in synthesis gas streams derived from coal or biomass ($H_2/CO = 1.0$) and optimized activation protocols for high activity, selectivity and mechanical integrity.
(3) determined the kinetic influence of the hydrogen and carbon monoxide partial pressure on catalytic rates and selectivities and propose mechanistic alternatives that can be used for further improvements of Fischer-Tropsch synthesis rates and selectivities.
(4) proposed a reaction mechanism in agreement with the experimental data. This mechanism can explain the pathways for hydrocarbons and carbon dioxide formation.
(5) analyzed and showed the concordance between the mechanism proposed and the kinetic consequences of using D_2/CO instead of H_2/CO.
(6) performed theoretical calculations about the validity of Fischer-Tropsch Synthesis mechanism proposed. A good agreement between the experimental data and the theoretical calculations has been found.
(7) explored the potential use of recently developed colloidal precipitation methods for the synthesis of more active and selective Fischer-Tropsch synthesis catalysts based on Fe and CO.

Further detailed results, findings, and conclusions are included in the last part of this report as sections:

2.1. Catalytic performance of Fe-Zn-Cu_3-K_6 in Fischer-Tropsch Synthesis.
2.2. Kinetic study of the Fischer-Tropsch Synthesis.
    2.2.1. Mechanism and kinetics.
    2.2.2. Kinetic H_2/D_2 isotope effects on Fe-based catalysts.
    2.2.3. Theoretical calculations for the Fischer-Tropsch Synthesis mechanism.
2.3. Metallic colloids for Fischer-Tropsch Synthesis catalysts.
    2.3.1. Effect of SiO_2 modification with ZrO_2.
    2.3.2. Effect of colloid method.

Detailed results, findings and conclusions

1. Experimental details

1.1. Synthesis of Precursors and Catalysts

The addition of promoters to Fe-Zn oxide precursors was accomplished following two different procedures, which are shown in Scheme 1. The aqueous solutions of K_2CO_3, $Cu(NO_3)_2$, or ruthenium (III) nitrosylnitrate $[Ru(NO)(NO_3)_x(OH)_y$ $(x+y = 3)]$ were used as the sources of K, Cu and Ru. The first process (Route 1) was carried out according to the previously reported work. First, potassium was added by incipient wetness impregnation with solutions with the required concentration to obtain the desired K/Fe atomic ratio (K/Fe = 0.06). Next the solid was dried overnight at 393 K in ambient air. Cu or Ru were then added at a Cu/Fe and Ru/Fe atomic ratio of 0.03 (Cu(Ru)/Fe = 0.03) in a second step, followed by overnight drying at 393 K in ambient air. Finally, the samples were treated in flowing dry air at 543 K for 4 h. The resulting oxide precursors are denoted throughout as Fe-Zn-K_6, Fe-Zn-K_6-Cu_3, and Fe-Zn-K_6-Ru_3, respectively. The other process (Route 2) was carried out as follows. First, Cu or Ru were added to the Fe-Zn oxide precursor at Cu(Ru)/Fe atomic ratios (Cu(Ru)/Fe = 0.03), followed by overnight drying at 393 K in ambient air and drying at 543 K for 4 h in flowing dry air. Potassium was then added at K/Fe atomic ratios (K/Fe = 0.06) in the second step, followed by overnight drying at 393 K in ambient air. These samples were again treated in flowing dry air at 543 K for 4 h. The resulting oxide precursors are denoted as Fe-Zn-Cu_3-K_6 and Fe-Zn-Ru_3-K_6, respectively.

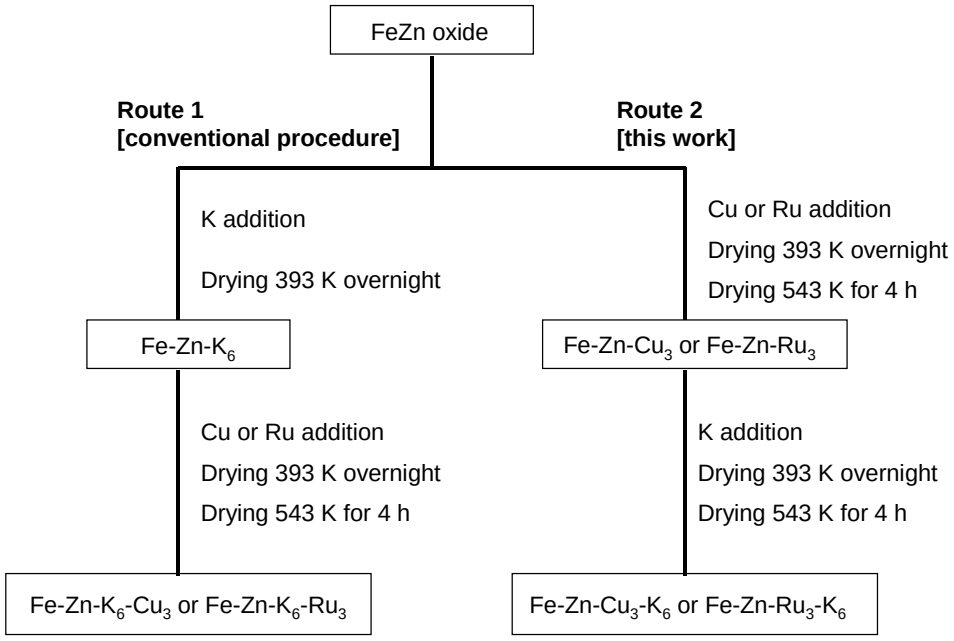

Scheme 1. Procedure for preparation of iron-based catalysts with promoters.

We have also studied the use of colloidal precipitation methods for the synthesis of small Fe and Co clusters using recently developed methods. Several catalytic samples has been prepared following the experimental procedures described below.

1. A ZrO_2/SiO_2 support (Zr density is 3.2 at. nm^{-2}) was prepared by impregnation of SiO_2 (Davison Grace 62, 287 m^2 g^{-1}, treated in dry air at 873 K for 16 h before use) with an aqueous zirconyl nitrate (Aldrich, 99.99%) in doubly distilled deionized water. The impregnation was carried out at 373 K in air. The soild was then treated in flowing dry air (Praxair, extra dry, 1.67 $cm^3 \cdot s^{-1}$) by heating from room temperature to 773 K at a rate of 0.17 $K \cdot s^{-1}$. The temperature was kept at 773 K for 3 h.

2. The preparation of a 11 wt.% Co/SiO_2 catalyst was carried out by incipient wetness impregnation of SiO_2 (Davison Grace 62, 287 m^2 g^{-1}, treated in dry air at 873 K for 16 h before use) with an aqueous solution of $Co(NO_3)_2 \cdot 6H_2O$ (Aldrich, 99.999%) in doubly distilled deionized water. The impregnation was carried out in four steps, with air dry at 373 K between them. The catalyst was treated in flowing dry air (Praxair, extra dry, 1.67 $cm^3 \cdot s^{-1}$) by heating from room temperature to 673 K at a rate of 0.17 $K \cdot s^{-1}$ and keeping constant the temperature for 4 h [1].

3. A 11 wt.% Co/SiO_2 catalyst was also prepared by using inverse micelles. Before the preparation, toluene and doubly distilled deionized (DDI) water solution were bubbled with Ar (Praxair) for 2 h in order to remove oxygen. 15 g of didodecyldimethylammonium bromide (DDAB, Aldrich, >98%) was dissolved in 104 mL of toluene (Aldrich) to form a 0.3 M micelle solution. $CoCl_2$ (0.13 g, Aldrich, 99.9%) was then added to the above solution and sonicated until the solid disappeared and a blue solution was obtained. $NaBH_4$ (1.13 g, Aldrich, 99.99%) was then added in 30 mL of DDI water to produce a 1 M solution using a separate beaker. This 1 M $NaBH_4$ solution was slowly added to the micelle solution with a vigorously stirring to reduce $CoCl_2$. A black colloid was formed and the mixture was stirred to ensure a complete reaction [2]. Subsequently, 0.5 g of SiO_2 was added to the obtained colloidal solution and stirred for 3 h. An acetone solution (Aldrich, 99%) was used to induce flocculation. The solid was then filtered. After use acetone and DDI water to remove the surfactant, the obtained solids were treated in flowing dry helium (Praxair, 1.67 $cm^3 \cdot s^{-1}$) by heating from room temperature to 573 K at 0.17 $K \cdot s^{-1}$ and holding for 3 h.

4. A $Co/ZrO_2/SiO_2$ catalyst was prepared by incipient wetness impregnation of the ZrO_2/SiO_2 support with an aqueous $Co(NO_3)_2 \cdot 6H_2O$ (Aldrich, 99.999%) in doubly distilled deionized water. The impregnation was carried out in four steps, with air dry at 373 K between them. The catalyst was treated in flowing dry air (Praxair, extra dry, 1.67 $cm^3 \cdot s^{-1}$) by heating from room temperature to 673 K at 0.17 $K \cdot s^{-1}$ and holding for 4 h. The cobalt content was kept as 11 wt.%.

5. Another 11 wt.% $Co/ZrO_2/SiO_2$ catalyst was prepared *via* a homogeneous precipitation process with urea. Typically, 0.72 g of urea (ACROS) and 1.2 g of $Co(NO_3)_2 \cdot 6H_2O$ (Aldrich, 99.999%) were added to 65 mL of doubly distilled deionized water. After the addition of 2 g of ZrO_2/SiO_2 (Zr density is 3.2 $at \cdot nm^{-2}$) support, the temperature of the solution was increased to 363 K and maintain at this value for 12 h. The obtained pink suspension was subsequently cooled down to ambient temperature and filtered. The solid was dried at 373 K in air and treated in flowing dry air (Praxair, extra dry, 1.67 $cm^3 \cdot s^{-1}$) by heating from room temperature to 673 K at 0.17 $K \cdot s^{-1}$ and holding for 4 h.

1.2. Catalysts characterization.

X-Ray diffraction (XRD) patterns were measured with a Siemens D5000 diffraction-meter using CuK_α radiation.

Temperature-programmed reduction (TPR) experiment was operated in a flow unit equipped with a thermal conductivity detector (QS-10, Quantachrome Corp.). The sample was placed inside a U-type quartz reactor and treated in 20 % H_2 (Praxair, 20% H_2, 80% Ar, 1.33 $cm^3\ s^{-1}$) by heating to 1123 K at a rate of 0.17 $K{\cdot}s^{-1}$. The TCD detector was calibrated by reducing CuO.

Chemisorption data were collected with a Quantachrome 1C Autosorb apparatus. The sample was reduced in pure hydrogen (Praxair) at 673 K for 1h and then evacuated at this temperature for 0.5 h to remove the chemisorbed hydrogen on the surface. The hydrogen chemisorption was carried out at 373 K (Quantasorb chemisorption analyzer). Adsorption isotherms were extrapolated to zero pressure to obtain the chemisorption uptakes. Dispersion values were calculated from hydrogen uptake and cobalt content assuming a 1:1 stoichiometry of H to surface cobalt atoms. The crystal diameter was calculated by using the equation d=96/D (D=dispersion), which assumes hemispherical crystallites with random surface orientation exposing low-index crystal planes.

1.3. Fischer-Tropsch Synthesis activity and selectivity

Fischer-Tropsch synthesis rates and selectivites were measured in a single-pass packed-bed reactor with plug-flow hydrodynamics. This reactor was held within a resistively-heated three-zone furnace. All lines after the reactor were kept at 433-553 K and a vessel placed immediately after the reactor was held at 408 K to collect liquid products. Reactant and product streams were analyzed online using a gas chromatograph (Agilent Technologies, model 6890N). The analysis of N_2, CO, CO_2, and CH_4 was performed using a thermal conductivity detector and a Porapak Q packed-column (15.2 cm × 0.318 cm diameter). All hydrocarbons up to C_{15} were analyzed on-line using flame ionization detection and a cross-linked methyl silicone capillary column (HP-1, 50 m×0.32 mm; 1.05 μm film).

Fe catalysts (100-180 μ, 0.4 g) were diluted with 11 g of quartz granules (100-180 μ) to avoid temperature gradients. Quartz granules were washed with concentrated nitric acid and treated in air at 973 K before use. Catalysts were activated using flowing synthesis gas ($H_2/CO = 2$) at 0.1 MPa by increasing the temperature from 298 to 423 K at a rate of 10 K/min and from 423 to 543 K at 1 K/min. The catalysts were held at 543 K for 1 h. After activation, the temperature was decreased to 508 K, and the synthesis gas ($H_2/CO = 1$) pressure was gradually increased to 2.14 MPa. FTS reactions were carried out with the synthesis gas (Praxair; $H_2/CO/N_2$ mixture; (i) 0.62/0.31/0.07 [$H_2/CO = 2$], or (ii) 0.46/0.46/0.08 mol [$H_2/CO = 1$]) as reactant at 2.14 MPa gas pressure and 508 K.

2. Results and Discussion

2.1. Catalytic performance of Fe-Zn-Cu_3-K_6 in the Fischer-Tropsch Synthesis

The procedure proposed in the previous reporting period for catalytic promoters addition leads to Fe-Zn-Cu_3-K_6 and Fe-Zn-Ru_3-K_6 catalysts with a superior FTS catalytic rates compared to those obtained with the Fe-Zn-K_6-Cu_3 and Fe-Zn-K_6-Ru_3 catalysts prepared by the conventional procedure. Besides, we have found that the Fe-Zn-Cu_3-K_6 catalyst showed the highest FTS performance among all the catalysts here studied.

Table 1 compares the FTS reaction rates and selectivities obtained with the Fe-Zn-Cu_3-K_6 sample at relatively high (H_2 + CO) conversions with those values reported in the literature with the most active Fe-based catalysts. These Fischer-Tropsch synthesis rates and selectivites were measured in a fixed-bed reactor. Synthesis gas with low H_2/CO ratio (H_2/CO = 1) led to low hydrocarbon productivities when compared with stoichiometric synthesis gas (H_2/CO = 2). Fe-Zn-Cu_3-K_6 showed the highest hydrocarbon productivity for FTS reaction among all reported catalysts, even though previously reported catalysts were tested at higher temperature.

Table 1. Steady-state FTS performance of various Fe-based catalysts in fixed-bed reactor.

	$FeZnCu_3K_6$ This work		$FePtK/SiO_2$[a] [3]	Fe/Cu/K[b] [4]
Temperature (K)	508	508	543	533
Pressure (MPa)	2.14	2.14	1.14	1.5
H_2/CO ratio	1.0	2.0	1.0	1.0
GHSV (NL/h/g-cat)	6.8	8.9	1.92	4.0
(H_2 +CO) conversion (%)	53.4	51.3	53.5	54.8
CO_2 selectivity (%)	36.6	28.1	39.7	45.0
Hydrocarbon productivity (g/h/g-cat)	0.65	0.79	0.1	0.43

a 10Fe/1.0Pt/0.2K/88.8SiO_2

b 100Fe/5Cu/4.2K

In Table 2, the FTS reaction rates and selectivities of Fe-Zn-Cu_3-K_6 samples in fixed-bed reaction are also compared with FTS performance reported in slurry reactor. The data for the slurry reactor have been obtained from the literature [5-7]. FTS reaction rates and selectivities on Fe-Zn-Cu_3-K_6 samples in fixed-bed reaction were measured at two different condition; (i), at 508 K, 2.14 MPa; and (ii), at 543 K, 1.31 MPa. Higher temperatures led to higher hydrocarbon productivities, despite the fact of the lower reactant pressures used. The hydrocarbon synthesis productivity on Fe-Zn-Cu_3-K_6 under synthesis

gas stream with $H_2/CO = 1.0$ at 543 K and 1.31 MPa was about 2 times higher than that reported on Fe-$Si_{4.6}$-$K_{1.4}$, even though Fe-Zn-Cu_3-K_6 was tested under a synthesis gas stream with a lower H_2/CO ratio ($H_2/CO = 1.0$ *versus* 1.7). These reported catalysts showed moderate activity in long period of reaction time (115–600 h) [5-7]. The sequence Fisher-Tropsch synthesis on Fe-Zn-Cu_3-K_6 was, therefore, carried out at 508 K and 2.14 MPa under synthesis gas stream (10.0 NL/h.g-cat.) with $H_2/CO = 1$ for 240 h in order to examine the stability of the catalyst.

Table 2. Steady-state FTS performance of various Fe-based catalysts using coal- or biomass-derived synthesis gas ($H_2/CO = 1.0$-1.7).

	$FeZnCu_3K_6$		FeK/SiO_2[a]	$FeCuK/SiO_2$[b]	$FeCuK/SiO_2$[c]
	This work		[5]	[6]	[7]
Reactor Type	Fixed-bed		Slurry	Slurry	Slurry
Temperature (K)	508	543	543	533	523
Pressure (MPa)	2.14	1.31	1.31	2.00	1.48
H_2/CO ratio	1.0	1.0	1.7	0.7	0.7
(H_2 +CO) conversion (%)	53.4	43.3	50.0	67.0	56.1
CO_2 selectivity (%)	36.6	41.1	40.0	–	41.1
Hydrocarbon productivity (g/h/g-cat)	0.65	1.91	1.00	0.16	0.37

a 100Fe/4.6Si/1.4K
b 100Fe/5Cu/3K/8SiO_2
c 100Fe/4.3Cu/4.1K/25SiO_2

Figure 1 shows the evolution of the CO conversion and hydrocarbon formation rate with the time-on-stream. The rates of CO conversion and hydrocarbon formation on Fe-Zn-Cu_3-K_6 decreased rapidly during an initial period (ca. 9 h). For the initial period, the fast decrease of FTS performance is probably attributed to the decrease of surface area as a consequence of the carbide-oxide transformations, accumulation of high-molecular-weight products (wax) in the catalyst pores, and changes in the catalyst composition as the reaction proceeds. Following this initial period, the activity continued to decline with time-on-stream, although the decrease of the reaction rate is much less accentuated. Thus, the CO conversion decreased from 35% at 10 h to 30% at 240 h on stream. Simultaneously, CO_2 selectivity, C_{5+} selectivity and olefin/paraffin ratio also decreased gradually during the reaction, while the amount of the light products formed on the catalyst increased gradually with increasing time on stream. The modest drop in activity may be attributed to several factors: (i), formation of inactive species such as carbon on the surface; (ii), loss of active sites due to sintering and/or fouling by products. It seems that the decrease of the hydrocarbon formation rates was caused by the disappearance of promoters from the

catalyst and/or by the removal of the catalyst itself from the bed, instead of deactivation of catalysts. This is supported by the fact that the waxes collected after the reactor displayed black color, suggesting that Fe carbides were probably mixed with the waxes. It has been reported that higher temperature and higher H_2/CO ratio improves the catalytic life [4,5]. The improvement of the experimental preparation method may result in more stable FTS rates on Fe-Zn-Cu_3-K_6.

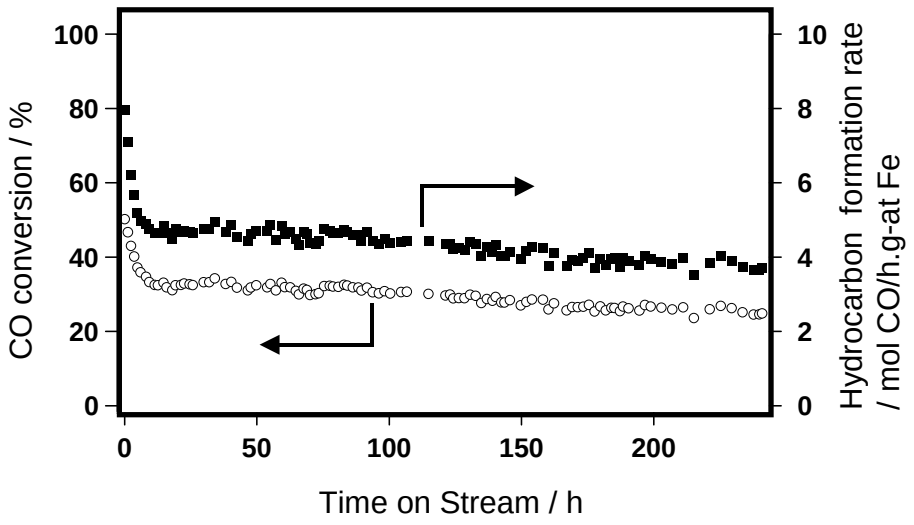

Figure 1. CO conversions and hydrocarbon formation rates with time on stream (H_2/CO = 1, SV=10.0 NL/h.g-cat.) at 508 K and 2.14 MPa.

In this project, we have reported that the effects of promoters (K, Cu, Ru) on Fisher-Tropsch synthesis rate and selectivity as well as the effect of two different procedures for promoter addition. The $FeZnCu_3K_6$ obtained by the effort in this project gave unprecedented activity and C_5^+ selectivity for hydrogen-poor synthesis gas (H_2/CO=1) reactant, and showed modest activity in long period of reaction time (240 h).

2.2. Kinetic Study of the Fischer-Tropsch Synthesis.

2.2.1. Mechanism and kinetics.

The kinetics of the Fischer-Tropsch Synthesis (FTS) have been studied during this reporting period. The kinetic measurements have been performed on Fe-Zn-Cu_3-K_6, which was found to be the most active catalyst in previous studies. The ultimate objective of these experiments is to propose a reaction mechanism that describes and predicts the rates of formation of the various hydrocarbons formed during reactions of CO and H_2 on Fe-based catalysts and which can be used to embed into hydrodynamic models of complex practical reactors.

In the previous reporting period, we proposed a set of elementary steps in which we considered two different pathways for CO activation:

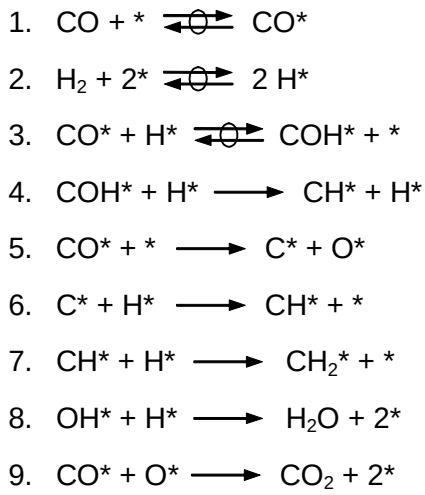

Scheme 2. Proposed elementary steps for hydrocarbons (CH_2* species), water and primary carbon dioxide formation from CO and H_2.

The validity of the proposed mechanism was tested by comparing the experimental and the calculated rates of hydrocarbons, primary CO_2 and water formation respectively. It was observed that the reaction rates calculated with the kinetic expressions derived from our model were in good agreement with the experimental values.

2.2.2. Kinetic H_2/D_2 isotope effects on Fe-based catalysts.

During this reporting period, we have analyzed the consistency between the mechanism we proposed and the H_2/D_2 kinetic isotope effect (r_H/r_D) over a conventional iron-based Fischer-Tropsch catalyst Fe-Zn-K-Cu. The reaction mechanism we have recently proposed for the Fischer-Tropsch Synthesis consists of parallel pathways for CO activation over Fe-based catalysts. On one hand, adsorbed carbon monoxide species (CO*) can be directly dissociated to form surface carbon atoms (C*) which can be subsequently hydrogenated to produce the FTS monomers (CH_2*). But at the same time, hydrogenation of carbon monoxide molecules associatively adsorbed leads also to the formation of surface monomers. Although both monomer formation routes occur simultaneously over the catalyst surface, our results showed that the hydrogen-assisted CO dissociation mechanism is predominant at typical H_2 and CO partial pressures. According to this mechanism, dihydrogen and hydrogen atoms formed *via* its dissociation are involved in all proposed elementary steps, except for the unassisted CO dissociation. Therefore, kinetic deuterium isotope effects could be use as a guide to determine the kinetically relevant steps and to support a specific mechanism because the rate constant for the reaction of the hydrogen compound (k_H) differs of that obtained for the same reaction with the corresponding deuterium compound (k_D) when a bond to hydrogen or deuterium is formed or broken in the kinetically-relevant steps of a reaction. On the other hand, the thermodynamic

deuterium isotope effect, namely, the effect of isotopic substitution on the equilibrium constant, can be used to indicate important characteristics of reaction equilibriums. Therefore, comparisons of rates and selectivities for reactions of H_2/CO and D_2/CO mixtures on iron-based catalysts can provide specific evidence about the nature of the kinetically-relevant steps.

Figures 2 shows the CO conversion rate to hydrocarbons as a function of the CO conversion level. It can be clearly seen that hydrocarbons formation rate is higher (about two times) when D_2/CO reactants mixture is used instead of H_2/CO reactants. It is also noted that hydrocarbon formation rate decreases when the CO conversion is increased.

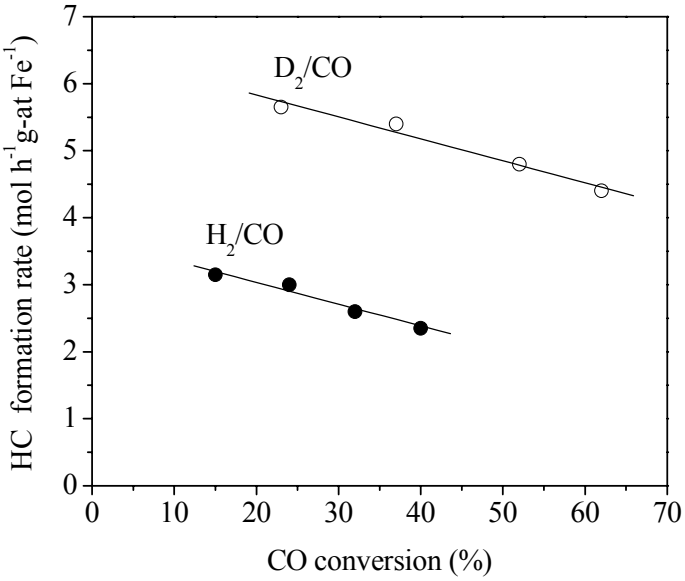

Figure 2. Hydrocarbon formation rate as a function of CO conversion for H_2/CO or D_2/CO reactants (Zn/Fe=0.1, K/Fe=0.02, Cu/Fe=0.01) at 508 K and 2.14 MPa.

The following rate expression for the CO conversion rate to hydrocarbons can be derived from these elementary steps assuming *pseudo*-steady-state for all adsorbed intermediates and *quasi*-equilibrium for steps 1, 2 and 3 in Scheme 2:

$$r_{CH_2} = \frac{K_1 K_2 K_3 k_4 P_{CO} P_{H_2} + K_1 k_5 P_{CO}}{(1 + K_1 P_{CO})^2}$$

where r_{CH_2} is the CO conversion rate to hydrocarbons, and k_i and K_i are respectively the rate coefficient and the equilibrium constant for step *i*. The observed kinetic isotope effect will be, therefore, the combination of the influence of hydrogen or deuterium use on K_2, K_3 and k_4. Since the first term of the numerator is about seven times higher than the second term, we can assume that the corresponding KIE will be proportional to the following expression:

$$KIE = \frac{r_{CH_2}}{r_{CD_2}} \propto \frac{K_2^H K_3^H k_4^H}{K_2^D K_3^D k_4^D} = \frac{K_2^H}{K_2^D} \cdot \frac{K_3^H}{K_3^D} \cdot \frac{k_4^H}{k_4^D}$$

where r_{CH_2} and r_{CD_2} is the CO conversion rate to hydrocarbons with H_2/CO and D_2/CO respectively, and the superscript of the rate coefficients and equilibrium constants is related to the hydrogen- or deuterium-containing syngas. Therefore, the observed isotope effect must be the result from the combination of kinetic and equilibrium isotope effects.

Figure 3 shows the rate of carbon dioxide formation with H_2/CO and D_2/CO reactants as a function of CO conversion at 508 K and 2.14 MPa. It can be observed that the CO_2 formation rates extrapolated to low CO conversion levels are non-zero, consistent with the primary pathway of oxygen removal as carbon dioxide (step 9 in Scheme 1) (27). This primary CO_2 formation rate is practically the same with D_2/CO or H_2/CO reactants. In other words, the use of D_2/CO or H_2/CO syngas has no effect on the oxygen removal process as carbon dioxide. This experimental observation agrees with the FTS mechanism depicted in Scheme 1. It can be demonstrated that the primary carbon dioxide formation rate is given by the following expression:

$$r^{p}_{CO_2} = \frac{K_1 k_5 P_{CO}}{(1 + K_1 P_{CO})^2}$$

According to this expression, the formation of carbon dioxide through primary pathways is not influenced by the use of D_2/CO or H_2/CO.

On the contrary, we have detected that deuterium affects the formation of carbon dioxide through secondary reactions. It is evident from Figure 3 that CO_2 formation rate increases with decreasing space velocity (and increasing reactor residence time and CO conversion). The slope of the CO_2 formation rate reflects the synthesis of CO_2 by reaction of water with CO-derived intermediated in secondary reactions with the stoichiometry of the water-gas shift reaction (WGS).

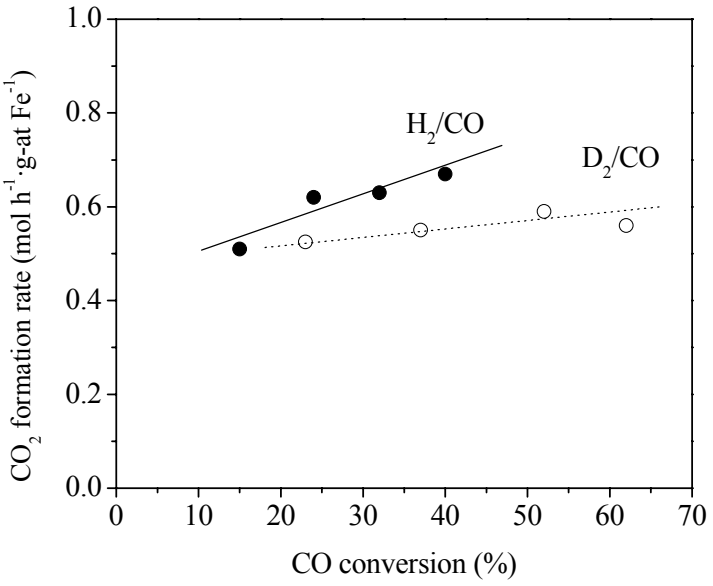

Figure 3. CO_2 conversion rate as a function of CO conversion for H_2/CO or D_2/CO reactants (Zn/Fe=0.1, K/Fe=0.02, Cu/Fe=0.01) at 508 K and 2.14 Mpa.

2.2.3. Theoretical calculations for the Fischer-Tropsch Synthesis mechanism.

During this reporting period, we have also developed some theoretical calculations about the Fischer-Tropsch Synthesis mechanism that we have proposed, as well as the corresponding kinetic isotope effect. This work has been done in close collaboration with Prof. Manos Mavrikakis, from the University of Wisconsin, Madison.

From these DFT calculations, we have demonstrated that the H-assisted CO dissociation pathway is energetically favored on a Fe(110) surface. Moreover, we have determined that the most probable intermediates are surface formyl species. These calculations and results support our hypothesis about the importance of the assistance of hydrogen species (H*) in the CO dissociation event. We have also found that the unassisted CO cleavage also takes place to some extent. Therefore, this is in accordance with the experimental observation consisting in the formation of primary carbon dioxide, which is produced via the unassisted CO pathway. On the contrary, we have found that the energy barrier for the unassisted CO dissociation route is much higher than the assisted one on a Co(0001) surface. Consequently, hydrocarbons formation occurs exclusively via the H-assisted pathway and no primary carbon dioxide is formed.

We have also carried out some theoretical calculations in order to explain the inverse kinetic isotope effect found experimentally when using D_2 instead of H_2.

Typically, it is supposed that in a chemical reaction, the bond-forming event takes place along the stretching mode of the bond being formed. Therefore, a regular primary KIE is expected, with the light isotope giving faster rates. In those cases, the dominant stretching mode is gone at the transition state complex, and as a result, the lighter element has a smaller barrier and gives higher rates. Assuming that the rate-determining step for hydrocarbons synthesis is the formation of formyl species (CO* + H* → HCO*), we have found that the event consisting in the H—CO formation does not occur along the H-C bond stretching mode, but along a "twist" mode, twisting H around CO. As a result, the highest frequency (C-H stretch), which dominates the ZPE corrections for the Initial and the Transition State, remain there for both states. We have calculated the theoretical value of the kinetic isotope effect for the formyl species formation. We have observed a good agreement between these calculation and the experimental value.

2.3. Metallic colloids for Fischer-Tropsch Synthesis catalysts

2.3.1. Effect of SiO_2 modification with ZrO_2.

Supported cobalt catalysts are well-known for their good performance in the Fischer–Tropsch Synthesis. In order to develop more active catalysts, much research effect has been taken to enhance the cobalt dispersion by decreasing the average particle size. However, it is demonstrated that irreducible mixed oxides species, such as cobalt silicate, are often formed when small sized cobalt are present on some type of oxidic supports, e.g. SiO_2, Al_2O_3 [8-10]. Such strong metal-oxide interactions not only mask the cobalt particle size effect, but also waste the active component. Loading a layer of ZrO_2 provides a simply but effective approach to modify the support surface properties, which might weaken the metal-support interaction [11]. Figure 4 shows the XRD pattern obtained with the ZrO_2/SiO_2 support. It displays a broad diffraction peak between 20 and 40 degrees,

indicating the formation of amorphous ZrO_2 on the SiO_2 surface. This result means that the present impregnation method enables to prepare a homogeneous ZrO_2 layer on the SiO_2 surface.

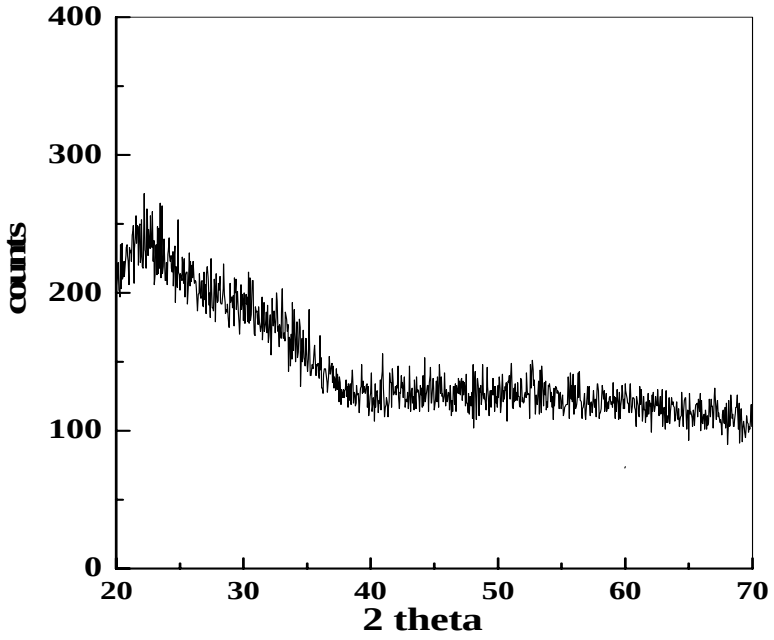

Figure 4. XRD pattern of the ZrO_2/SiO_2 support.

Table 3 shows the H_2-chemisorption results with the cobalt-supported catalysts. Although the calculated cobalt particle size is quite large (>20nm) for both samples, it is obvious that the use of ZrO_2/SiO_2 as support leads to a decrease of the cobalt crystal size, resulting in solid with a better dispersion than Co/SiO_2. The reduction behavior of supported cobalt catalysts was examined by H_2-TPR (Figure 5). Similarly to the literature reports, the reduction of as-treated cobalt oxide supported sample to its metal crystallites requires two step leading to distinct peaks in the TPR profiles. In the first step, Co_3O_4 is reduced to CoO. These species are further reduced to Co metal at higher temperatures, resulting in a broader peak in the second step [1]. As shown in Table 4, the calculated the H_2/Co ratio is close to the theoretical values, suggesting that almost all the cobalt oxide species can be reduced to metal crystallites at a temperature region of 470-750 K. Comparatively, it is obvious in Figure 2 that the cobalt-supported ZrO_2/SiO_2 sample exhibits a lower reduction temperature than the Co/SiO_2 catalyst.

Table 3. H_2-chemisorption results.

Sample	Co dispersion (%)	Average Cobalt size (nm)
11 wt.% Co/SiO_2	3.1	31
11 wt.% $Co/ZrO_2/SiO_2$,	4.2	23

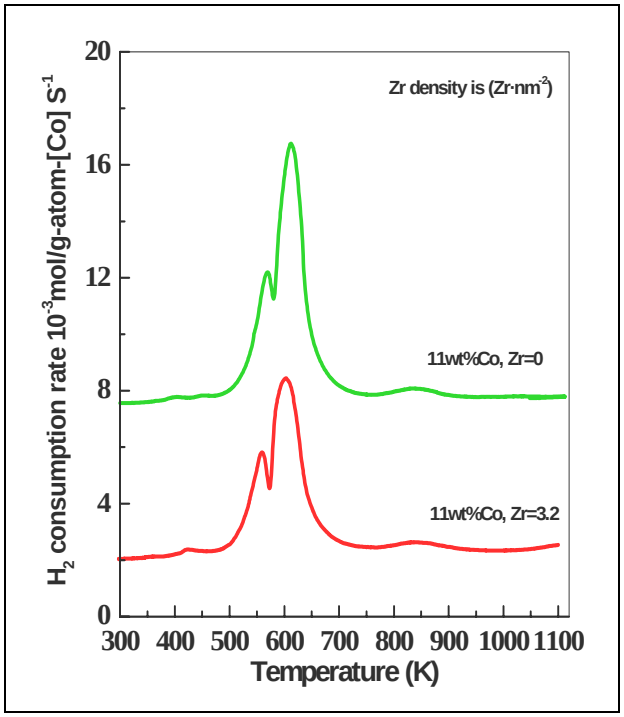

Figure 5. H_2-TPR profiles of 11 wt.% Co-supported on SiO_2 and ZrO_2/SiO_2, respectively, prepared by incipient wetness impregnation.

Table 4. Assignments of reduction peaks reported in Figure 5.

Sample	Reduction temperature (K)	Assignment	H_2/Co-species (theoretical values are given in parentheses)
11 wt.% Co/SiO_2	480-581	from Co_3O_4 to CoO	0.28 (0.33)
	581-750	from CoO to Co	1.04 (1.00)
11 wt.% $Co/ZrO_2/SiO_2$	470-574	from Co_3O_4 to CoO	0.33 (0.33)
	574-735	from CoO to Co	1.05 (1.00)

2.3.2. Effect of colloid method.

The preparation of transition metallic nanoparticles by the colloid methodology is a very attractive route to prepare metal or bimetal supported catalysts because it provides an opportunity to control the metal particle structure, size, shape as well as the metal dispersion, which significantly affects the catalytic performance (activity and selectivity) [12,13]. In this study, we have successfully prepared a stable cobalt colloid via inverse micelle method, and load it on the SiO_2 support. Based on the TEM results (Figure 6a), small spherical particles with homogeneous size distribution (3-5 nm) can be prepared according to developed method. These small nanoparticles are ascribed to crystallized cobalt relevant species, e.g., CoO, Co_2B (HRTEM in Figure 6b). These results were confirmed by X-ray diffraction characterization (Figure 7), which exhibits a small but broad diffraction peak around 45°. However, it is difficult to ascribe this peak to Co_2B (XRD peak at 45.7°) or Co metal (XRD peak at 44.4°) [14,15]. Although the application of

$NaBH_4$ allows to form stable and small sized metallic crystals in the liquid phase directly, it bring the inorganic impurities, e.g. Na, B in the catalyst leading to unclean particle surface.

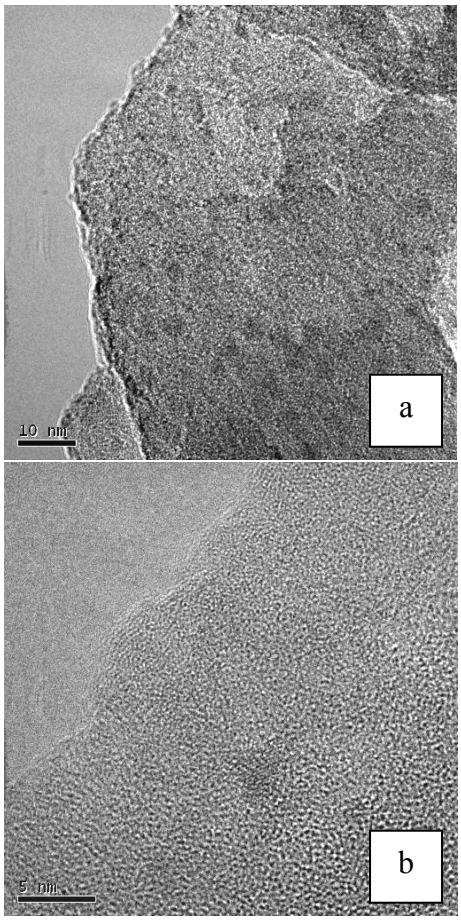

Figure 6. TEM pictures of 11 wt.% Co/SiO_2 prepared by inverse micelle method.

In order to avoid the impurities, urea was applied instead of $NaBH_4$. Although it unable to reduce the cobalt salts to crystallites in the liquid phase, the slowly decomposition of this base under desired temperature condition would increase pH value of solution, resulting in homogeneous precipitate cobalt nitrate to cobalt hydroxide or cobalt oxyhydroxide species [16]. This process also allows to obtain small cobalt particles on the support after high temperature treatment. However, the H_2-TPR characterization results (Figure 8) shows that the formed cobalt species interact strongly with the support ZrO_2/SiO_2, leading to large amount of cobalt silicate species difficult to reduce (the reduction peak is higher than 900K and the H_2/Co ratio is 0.69). The present results suggest that the cobalt precursor nature has a significant influence on the final catalyst. In contrast to conventional incipient wetness impregnation method, although the present colloidal synthesis approaches enables to prepare small cobalt particles, it often forms amount of hard reducible cobalt silicate species. To prepare a high-dispersed cobalt supported catalyst with easy reduction property, the cobalt precursor property (e.g. species and structure) is also critical in addition to the modification of support.

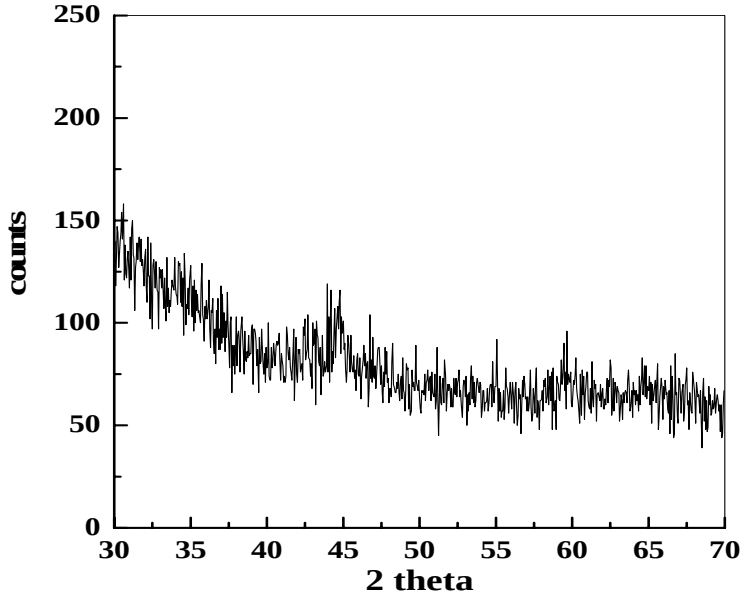

Figure 7. XRD pattern of Co/SiO_2 prepared by inverse micelle method.

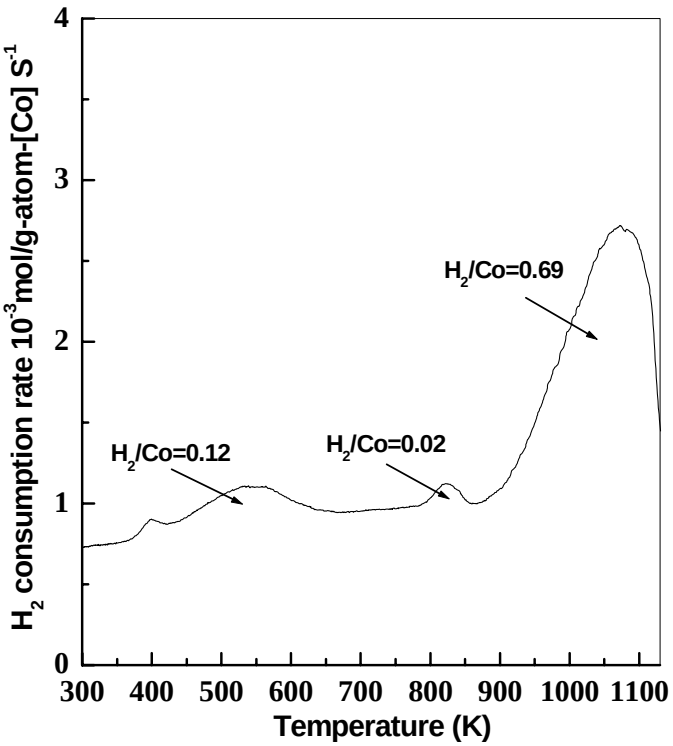

Figure 8. H_2-TPR picture of $Co/ZrO_2/SiO_2$ (11 wt.% Co, Zr density is 3.2 $Zr{\cdot}nm^{-2}$) sample prepared via urea homogeneous precipitation

References

[1] E. Iglesia, S. L. Soled, R. A. Fiato, G. H. Via, J. Catal. 143 (1993) 345.

[2] X.M. Lin, C.M. Sorensen, K.J. Klabunde, G.C. Hadjipanayis, Langmuir 14 (1998) 7140.

[3] J. Xu, C.H. Bartholomew, J. Sudweeks, D.L. Eggett, Topics Catal. 26 (2003) 55.[4] D.B. Bukur, X. Lang, D. Mukesh, W.H. Zimmerman, M.P. Rosynek, C. Li, Ind. Eng. Chem. Res. 29 (1990) 1588.

[5] A.P. Raje, R.O' Brien, B. H. Davis, J. Catal. 180 (1998) 36.

[6] B. Wu, L. Bai, Z. Zhang, H. Xiang, Y. W. Li, Fuel 83 (2004) 205.[7] D.B. Bukur, S.A. Patel, X. Lang, Appl. Catal. 61 (1990) 329.[8]. J.L. Li, G. Jacobs, T. Das, Y.Q. Zhang, B. Davis, Appl. Catal. A 236 (2002) 67.

[9] G. Jacobs, P.M. Patterson, Y.Q. Zhang, T. Das, J. L. Li, B. Davis, Appl. Catal. A 233 (2002) 215.

[10] P.J. van Berge, J. van de Loosdrecht, S. Barradas, A.M. van der Kraan, Catal. Today 58 (2000) 321.

[11] A. Hoek, M.F.M. Post, J.K. Minderhoud, P.W. Lednor, U.S. Patent 4499209 (Shell Oil Company).

[12] R. Narayanan, M.A. El-Sayed, J. Catal. 234 (2005) 348.

[13] H. Einaga, M. Harada, Langmuir 21 (2005) 2578.

[14] G.N. Glavee, K.J. Klabunde, C.M. Sorensen, G.C. Hadjipanayis, Langmuir 9 (1993) 162.

[15] G.N. Glavee, K.J. KIabunde, C.M. Sorensen, G.C. Hadjipanayis, Inorg. Chem. 32 (1993) 414411.

[16] G.L. Bezemer, P.B. Radstake, V. Koot, A.J. Van Dillen, J.W. Geus, K.P. de Jong, J. Catal. 237 (2006) 291.

Appendix B:

1. Publications

1.1 A manuscript titled "Fischer-Tropsch synthesis on iron-based catalysts with hydrogen-poor synthesis gas" is currently under review by Prof. Iglesia and will be submitted for publication.

1.2 A manuscript titled "Structure Evolution and Spectroscopic Studies of Site Requirements in Iron-Catalyzed Fischer-Tropsch synthesis" is currently in preparation and will be submitted for publication.

1.3. A manuscript titled "A kinetic and mechanistic study of the Fischer-Tropsch Synthesis with Fe-based catalysts" is currently under review by Prof. Iglesia and will be submitted for publication.

2. Presentations and Abstracts

2.1. Akio Ishikawa, Manuel Ojeda, Enrique Iglesia, "Design, Synthesis and Catalytic Properties of Iron-Based Catalysts for the Synthesis Gas Conversion to Fuels and Chemicals", The Fifth Tokyo Conference on Advanced Catalytic Science and Technology (TOCAT 5), July 23 -28, 2006.

2.2. Manuel Ojeda, Akio Ishikawa, Enrique Iglesia, Rahul Nabar, Manos Mavrikakis, "Iron-Catalyzed Fischer-Tropsch Synthesis: Mechanism and Catalyst Optimization", AIChE 2006 Annual Meeting San Francisco, November 12-17, 2006.

2.3. M. Ojeda, R. Nabar, A. Ishikawa, A. Nilekar, M. Mavrikakis, E. Iglesia, "On the Fischer-Tropsch Synthesis reaction mechanism on Fe and Co catalysts", 8th Natural Gas Conversion Symposium, Natal, Brazil, May 27-31, 2007.